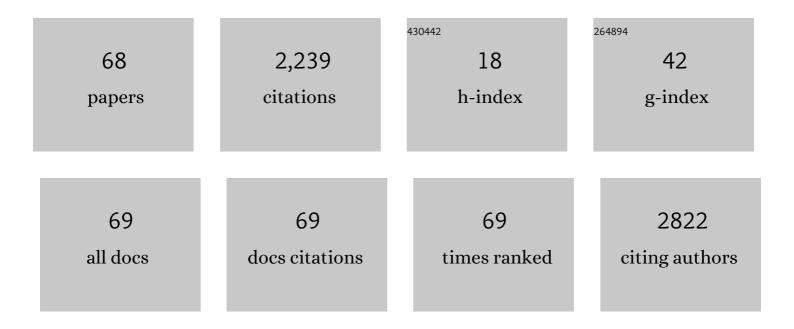
List of Publications by Year in descending order

Source: https://exaly.com/author-pdf/6327651/publications.pdf Version: 2024-02-01



MENC ZHANC

#	Article	IF	CITATIONS
1	Black phosphorus ink formulation for inkjet printing of optoelectronics and photonics. Nature Communications, 2017, 8, 278.	5.8	311
2	Multiple-Mode Orthogonal Frequency Division Multiplexing With Index Modulation. IEEE Transactions on Communications, 2017, 65, 3892-3906.	4.9	261
3	Solution processed MoS2-PVA composite for sub-bandgap mode-locking of a wideband tunable ultrafast Er:fiber laser. Nano Research, 2015, 8, 1522-1534.	5.8	256
4	2D Black Phosphorus Saturable Absorbers for Ultrafast Photonics. Advanced Optical Materials, 2019, 7, 1800224.	3.6	235
5	Black Phosphorus Based All-Optical-Signal-Processing: Toward High Performances and Enhanced Stability. ACS Photonics, 2017, 4, 1466-1476.	3.2	173
6	MXene Ti ₃ C ₂ T <i>_x</i> : A Promising Photothermal Conversion Material and Application in Allâ€Optical Modulation and Allâ€Optical Information Loading. Advanced Optical Materials, 2019, 7, 1900060.	3.6	115
7	102 fs pulse generation from a long-term stable, inkjet-printed black phosphorus-mode-locked fiber laser. Optics Express, 2018, 26, 12506.	1.7	104
8	A general ink formulation of 2D crystals for wafer-scale inkjet printing. Science Advances, 2020, 6, eaba5029.	4.7	89
9	MZIâ€Based Allâ€Optical Modulator Using MXene Ti ₃ C ₂ T <i>_x</i> (T =)	Tj ETQq1 :	1 0.784314 rg
10	A bismuthene-based multifunctional all-optical phase and intensity modulator enabled by photothermal effect. Journal of Materials Chemistry C, 2019, 7, 871-878.	2.7	67
11	Anisotropic Plasmonic Nanostructure Induced Polarization Photoresponse for MoS ₂ â€Based Photodetector. Advanced Materials Interfaces, 2020, 7, 1902179.	1.9	41
12	A Dual-Hop Virtual MIMO Architecture Based on Hybrid Differential Spatial Modulation. IEEE Transactions on Wireless Communications, 2016, 15, 6356-6370.	6.1	39
13	Allâ€Optical Control of Microfiber Knot Resonator Based on 2D Ti ₂ CT <i>_x</i> MXene. Advanced Optical Materials, 2020, 8, 1900977.	3.6	39
14	Wideband saturable absorption in metal–organic frameworks (MOFs) for mode-locking Er- and Tm-doped fiber lasers. Nanoscale, 2020, 12, 4586-4590.	2.8	36
15	MXene-based high-performance all-optical modulators for actively Q-switched pulse generation. Photonics Research, 2020, 8, 1140.	3.4	30
16	Antifouling mechanism of the additive-free β-PVDF membrane in water purification process: Relating the surface electron donor monopolarity to membrane-foulant interactions. Journal of Membrane Science, 2020, 601, 117873.	4.1	27
17	Signal processing assisted Vernier effect in a single interferometer for sensitivity magnification. Optics Express, 2021, 29, 11570.	1.7	27
18	High Sensitivity Fiber-Optic Strain Sensor Based on Modified Microfiber-Assisted Open-Cavity Mach-Zehnder Interferometer. Journal of Lightwave Technology, 2021, 39, 4556-4563.	2.7	24

#	Article	IF	CITATIONS
19	Environmentally stable black phosphorus saturable absorber for ultrafast laser. Nanophotonics, 2020, 9, 2445-2449.	2.9	21
20	Silicon hybrid plasmonic microring resonator for sensing applications. Applied Optics, 2015, 54, 7131.	2.1	18
21	Broad bandwidth dual-wavelength fiber laser simultaneously delivering stretched pulse and dissipative soliton. Optics Express, 2020, 28, 6937.	1.7	17
22	Pre-Coding Aided Differential Spatial Modulation. , 2015, , .		16
23	Microfluidic paper-based chip for parathion-methyl detection based on a double catalytic amplification strategy. Mikrochimica Acta, 2021, 188, 438.	2.5	16
24	Spatial-Modulation-Based Wireless-Powered Communication for Achievable Rate Enhancement. IEEE Communications Letters, 2017, 21, 1365-1368.	2.5	15
25	A few-layer InSe-based sensitivity-enhanced photothermal fiber sensor. Journal of Materials Chemistry C, 2020, 8, 132-138.	2.7	15
26	Hybrid plasmonic microcavity with an air-filled gap for sensing applications. Optics Communications, 2016, 380, 6-9.	1.0	14
27	Sub-150 fs dispersion-managed soliton generation from an all-fiber Tm-doped laser with BP-SA. Optics Express, 2020, 28, 34104.	1.7	12
28	Tapered-open-cavity-based in-line Mach–Zehnder interferometer for highly sensitive axial-strain measurement. Optics Express, 2022, 30, 6341.	1.7	10
29	Meridian whispering gallery modes sensing in a sessile microdroplet on micro/nanostructured superhydrophobic chip surfaces. Microfluidics and Nanofluidics, 2019, 23, 1.	1.0	9
30	Light sheet fluorescence microscopy applied for in situ membrane fouling characterization: The microscopic events of hydrophilic membrane in resisting DEX fouling. Water Research, 2020, 185, 116240.	5.3	9
31	Differential spatial modulation for dual-hop amplify-and-forward relaying. , 2015, , .		8
32	Spatial modulation orthogonal frequency division multiplexing with subcarrier index modulation for V2X communications. , 2016, , .		8
33	A Tunable Optical Bragg Grating Filter Based on the Droplet Sagging Effect on a Superhydrophobic Nanopillar Array. Sensors, 2019, 19, 3324.	2.1	8
34	Fiber-based all-optical modulation based on two-dimensional materials. 2D Materials, 2021, 8, 012003.	2.0	8
35	High quality factor multi-layer symmetric hybrid plasmonic microresonator for sensing applications. Optics Communications, 2017, 403, 68-72.	1.0	7

#	Article	IF	CITATIONS
37	Multiwavelength, subpicosecond pulse generation from a SWNT-SA mode-locked ring birefringent fiber laser. , 2015, , .		6
38	Quadrature index modulated OFDM with interleaved grouping for V2X communications. , 2016, , .		5
39	High-Q BSW-whispering gallery modes in periodic multi-layer microring resonator. Optics Communications, 2018, 410, 479-482.	1.0	5
40	2D Xenes: from fundamentals to applications. Nanophotonics, 2020, 9, 1555-1556.	2.9	4
41	Two-dimensional material as a saturable absorber for mid-infrared ultrafast fiber laser. Wuli Xuebao/Acta Physica Sinica, 2020, 69, 188101.	0.2	4
42	Four-wave mixing in graphdiyne-microfiber based on synchronized dual-wavelength pulses. Photonics Research, 2022, 10, 503.	3.4	4
43	Erbium-Doped Fiber Lasers Operated in a Strong Normal Dispersion Regime at Low Repetition Rate. IEEE Photonics Technology Letters, 2010, 22, 1401-1403.	1.3	3
44	Enhanced permeate flux by air micro-nano bubbles via reducing apparent viscosity during ultrafiltration process. Chemosphere, 2022, 302, 134782.	4.2	3
45	Ultra-low repetition rate all-normal-dispersion linear-cavity mode-locked fiber lasers. , 2009, , .		2
46	Chinese Semantic Role Labeling with Hierarchical Semantic Knowledge. , 2010, , .		2
47	Composite right/left-handed frequency-scanning antenna based on half mode substrate integrated waveguide. , 2016, , .		2
48	Hyperspectral scanning laser optical tomography. Journal of Biophotonics, 2019, 12, e201800221.	1.1	2
49	Ytterbium-doped mode-locked fiber laser at hundreds of kHz repetition rate. , 2009, , .		2
50	In situ visualization of combined membrane fouling behaviors using multi-color light sheet fluorescence imaging: A study with BSA and dextran mixture. Journal of Membrane Science, 2022, 649, 120385.	4.1	2
51	Ultra-low repetition rate SESAM-mode-locked linear-cavity erbium-doped fiber laser. , 2009, , .		1
52	Advances in SESAM and carbon nanotube saturable absorber mode locked fiber lasers. , 2009, , .		1
53	Broadband SESAM for mode locked Yb:fiber lasers. Science Bulletin, 2011, 56, 1348-1351.	1.7	1
54	Simplified calculation on the time performance of high efficiency frame generation algorithm in Advanced Orbiting Systems. , 2013, , .		1

#	Article	IF	CITATIONS
55	Mode and sensing properties of a silicon-based hybrid plasmonic microring resonator. Journal of Optics (India), 2019, 48, 308-313.	0.8	1
56	A simple and accurate measurement of fiber time delay in free-running linear-cavity laser configuration. , 2009, , .		0
57	Sub-100khz repetition rate mode-locked dispersion managed erbium-doped fiber laser. , 2009, , .		Ο
58	Phase shift compensation of high modulation depth multi-layer InGaAs/InAlAs SESAM. , 2009, , .		0
59	381 KHz repetition-rate operation of an ytterbium-doped fiber laser. , 2009, , .		0
60	Simplified cavity for erbium-doped fiber laser mode locked with spectral filtering. , 2009, , .		0
61	Analyzing the influence of electromagnetic parameters of composite material on antenna operating and coupling degree. , 2016, , .		0
62	Compressive holoscopy for 3D high resolution optical imaging acquisition with a single pixel detector. , 2017, , .		0
63	Wideband tunable ultrafast fiber laser using blackphosphorus saturable absorber. , 2017, , .		0
64	Observation of tunable dual-wavelength in a fiber laser mode-locked by black phosphorus. , 2017, , .		0
65	A Tunable Optical Filter Based on the Electrowetting Controlled Sagging Effect of a Liquid Droplet on a Superhydrophobic Substrate Embedding a Waveguide Bragg Grating. , 2019, , .		0
66	2D Materials for laser applications. , 2020, , 79-103.		0
67	Numerical analysis of low-RI WGM resonators excited by a periodically arranged multilayer dielectric planar waveguide. Optics Communications, 2021, 501, 127343.	1.0	0
68	Q-switched pulse generation in Yb- and Er-doped fiber laser with WS2 saturable absorber. , 2015, , .		0